2016

Dissociation of metabolic and hemodynamic levodopa responses in the 6-hydroxydopamine rat model

R. P. Lerner
Zucker School of Medicine at Hofstra/Northwell

Z. Bimpisidis

S. Agorastos

S. Scherrer

S. L. Dewey
Zucker School of Medicine at Hofstra/Northwell

See next page for additional authors

Authors
R. P. Lerner, Z. Bimpisidis, S. Agorastos, S. Scherrer, S. L. Dewey, M. A. Cenci, and D. Eidelberg

HHS Public Access

Author manuscript

Neurobiol Dis. Author manuscript; available in PMC 2017 December 01.

Published in final edited form as:

Neurobiol Dis. 2016 December ; 96: 31–37. doi:10.1016/j.nbd.2016.08.010.

Dissociation of Metabolic and Hemodynamic Levodopa Responses in the 6-Hydroxydopamine Rat Model

Renata P. Lerner[a], **Zisis Bimpisidis**[b], **Stergiani Agorastos**[a], **Sandra Scherrer**[a], **Stephen L. Dewey**[a], **M. Angela Cenci**[b], and **David Eidelberg**[a,*]

Renata P. Lerner: rlerner@nshs.edu; Zisis Bimpisidis: zisis.bimpisidis@med.lu.se; Stergiani Agorastos: sagorastos1@gmail.com; Sandra Scherrer: sassyhippy76@gmail.com; Stephen L. Dewey: sdewey@nshs.edu; M. Angela Cenci: angela.cenci_nilsson@med.lu.se

[a]Center for Neurosciences, The Feinstein Institute for Medical Research, Manhasset, NY 11030, USA

[b]Basal Ganglia Pathophysiology Unit, Department of Experimental Medical Science, Lund University, Lund, Sweden

Abstract

Dissociation of vasomotor and metabolic responses to levodopa has been observed in human subjects with Parkinson's disease (PD) studied with PET and in autoradiograms from 6-hydroxydopamine (6-OHDA) rat. In both species, acute levodopa administration was associated with increases in basal ganglia cerebral blood flow (CBF) with concurrent reductions in cerebral metabolic rate (CMR) for glucose in the same brain regions. In this study, we used a novel dual-tracer microPET technique to measure CBF and CMR levodopa responses in the same animal. Rats with unilateral 6-OHDA or sham lesion underwent sequential ^{15}O-water (H_2 ^{15}O) and ^{18}F-fluorodeoxyglucose (FDG) microPET to map CBF and CMR following the injection of levodopa or saline. A subset of animals was separately scanned under ketamine/xylazine and isoflurane to compare the effects of these anesthetics. Regardless of anesthetic agent, 6-OHDA animals exhibited significant dissociation of vasomotor (ΔCBF) and metabolic (ΔCMR) responses to levodopa, with stereotyped increases in CBF and reductions in CMR in the basal ganglia ipsilateral to the dopamine lesion. No significant changes were seen in sham-lesioned animals. These data faithfully recapitulate analogous dissociation effects observed previously in human PD subjects scanned sequentially during levodopa infusion. This approach may have utility in the assessment of new drugs targeting the exaggerated regional vasomotor responses seen in human PD and in experimental models of levodopa-induced dyskinesia.

Keywords

Parkinson's disease; microPET; cerebral blood flow; glucose metabolism; levodopa treatment

[*]**Corresponding author:** David Eidelberg, MD, Center for Neurosciences, The Feinstein Institute for Medical Research, 350 Community Drive, Manhasset, NY 11030, USA, Phone: 1-516-562-2498; Fax: 1-516-562-1008; david1@nshs.edu.

Introduction

A number of early studies were conducted to examine the vasomotor effects of dopaminergic drugs in animal models and human subjects (Leenders et al., 1985; McCulloch and Edvinsson, 1980). Studies in different species showed that the action of these agents was mediated by dopamine receptors on cerebrovascular smooth muscle cells (Edvinsson et al., 1978; Toda, 1976) and on neighboring astrocytes (Ruscher et al., 2012). Dopamine binding at these sites regulates vasomotor tone in a reversible, dose-dependent manner and maintains local neurovascular coupling (Edvinsson et al., 1985; Filosa et al., 2016; Guell et al., 1982).

The regional cerebrovascular effects of levodopa are noteworthy. This molecule crosses the blood brain barrier (BBB) through endothelial cells on brain capillaries. Studies in 6-hydroxydopamine (6-OHDA) rat models have found that chronic treatment induces changes in these blood vessels potentially altering BBB permeability and transport kinetics (Lindgren et al., 2009; Ohlin et al., 2011; Ohlin et al., 2012; Westin et al., 2006). Of note, these microvascular changes were observed mainly in chronically levodopa-treated animals developing abnormal dyskinetic movements in response to drug. Indeed, abnormal central handling of exogenously administered levodopa is regarded as the critical upstream trigger for these movements (Cenci, 2014).

Dissociation of neuronal and vasomotor effects has been reported as a consistent feature of acute levodopa administration in human Parkinson's disease (PD). We used dual-tracer imaging with ^{15}O-water (H_2 ^{15}O) and ^{18}F-fluorodeoxyglucose (FDG) PET in human PD subjects to monitor the changes in regional cerebral blood flow (CBF) and cerebral metabolic rate for glucose (CMR) that occurred during acute levodopa administration (Hirano et al., 2008; Jourdain et al., 2015). In these individuals, intravenous levodopa infusion lowered local CMR in the putamen, globus pallidus (GP)/subthalamic nucleus, ventral thalamus, and dorsal pons – areas with abnormally elevated metabolic activity in the baseline unmedicated ("off") condition (Asanuma et al., 2006). By contrast, CBF measurements acquired concurrently in the same subjects during drug infusion revealed consistent dissociation of the vasomotor (ΔCBF) and metabolic (ΔCMR) levodopa responses, with increases, rather than reductions in the treatment ("on") condition (Hirano et al., 2008). While localized dissociation was not seen during comparably efficacious STN stimulation, these effects were found to be exaggerated in PD subjects with levodopa-induced dyskinesia (LID) (Hirano et al., 2008; Jourdain et al., 2015).

An autoradiographic study of levodopa-mediated changes in regional CBF and glucose utilization was conducted in different groups of 6-OHDA lesioned rats (Ohlin et al., 2012). Whereas large increases in regional CBF were seen in the basal ganglia following levodopa administration, corresponding changes in regional glucose utilization were modest or altogether absent. While the autoradiographic findings are compatible with earlier observations in the human, levodopa-mediated dissociation in the rodent cannot be fully evaluated with this approach. Indeed, to localize and quantify levodopa-mediated dissociation in the rodent model, concurrent CBF and CMR measurements are needed from single animals scanned both at baseline and following administration of drug. To this end, we modified the dual-tracer approach for use in small animals scanned with microPET

before and after levodopa administration. Rats with unilateral 6-OHDA lesions were scanned with $H_2{}^{15}O$ and FDG microPET to map CBF and CMR at baseline and following the injection of levodopa or saline. Whole brain voxel-wise searches were conducted to identify regions with significant dissociation of vasomotor and metabolic responses to acute levodopa administration. In the first set of studies, scanning was performed under ketamine/xylazine anesthesia. Ketamine has been shown variably to affect regional CBF and CMR measurements in the rat brain (e.g., Cavazzuti et al., 1987). We therefore performed a set of microPET studies under isoflurane to determine whether levodopa-mediated dissociation effects were influenced by the choice of anesthetic agent.

Materials and Methods

Subjects

A total of 41 female Sprague-Dawley rats (200–350 g; Harlan, The Netherlands) were housed with one littermate per cage under a 12 h light/dark cycle with access to food and water *ad libitum*. All procedures were performed in accordance with the National Institutes of Health Guide for the Care and Use of Laboratory Animals and approved by the Institutional Animal Care and Use Committee (IACUC) at The Feinstein Institute for Medical Research in Manhasset, NY and by the Malmo-Lund Ethical Committee on Animal Research in Lund, Sweden.

Treatment Groups and Experimental Design

Ketamine/Xylazine—Rats with a unilateral 6-OHDA lesion of the medial forebrain bundle (n=20) or a sham lesion (n=21) received a single subcutaneous injection of levodopa or saline (1.0 mL/kg body weight) 30 minutes prior to anesthetic induction with ketamine and scanning on the Siemens Inveon (Siemens AG, Munich, Germany) microPET system at The Feinstein Institute for Medical Research.

Isoflurane—A subgroup of the ketamine animals were restudied under isoflurane anesthesia in two additional scanning sessions, each conducted at least one week after the other. The isoflurane animals had either unilateral 6-OHDA (n=8) or sham (n=7) lesion. In the first session, a subcutaneous saline injection (1.0 mL/kg body weight) was administered 30 minutes prior to anesthesia and subsequent brain imaging. In the second session, the animals received subcutaneous levodopa/benserazide 30 minutes prior to anesthesia and subsequent imaging.

Drugs

L-3,4-dihydroxyphenylalanine (levodopa) methyl ester and the peripheral decarboxylase inhibitor benserazide-HCl (Sigma-Aldrich, Stockholm, Sweden) were dissolved in saline and co-administered subcutaneously at the doses of 10/15 mg/kg. The injection volume was 1.0 mL/kg body weight.

Surgical Procedure

Dopamine-Denervating Lesion and Behavioral Screening—Rats received a unilateral injection of 6-OHDA-HCl (Sigma-Aldrich, Stockholm, Sweden) into the right

ascending dopamine fiber bundle (medial forebrain bundle). Rats were anesthetized with an intraperitoneal injection of a 20:1 mixture of fentanyl and medetomidine (Apoteksbolaget AB, Stockholm, Sweden) and placed in a stereotaxic frame. 6-OHDA was dissolved in a solution of 0.02% ascorbic acid/saline (3.5 μg/μL) and injected at the following two sites in accordance with standard protocol (i) 2.5 μL at anteroposterior (AP)=−4.4, lateral (L)= −1.2, dorsoventral (DV)= −7.8; toothbar=−2.4; (ii) 2.0 μL at AP=−4.0, L=−0.8, DV=−8.0; tooth bar=+3.4 (coordinates in mm relative to Bregma) (Ohlin et al., 2012). Sham lesions were performed by injecting saline at the same coordinates as the 6-OHDA procedures.

Two weeks following surgical lesion, rats were tested for amphetamine-induced rotation (2.5 mg/kg D-amphetamine intraperitoneally; 90 min recordings). Only animals exhibiting >5 net full turns per minute in the direction ipsilateral to the lesion were selected for the experiments (Winkler et al., 2002). The extent of the lesion was verified with tyrosine hydroxylase immunohistochemistry in all animals at the conclusion of the study. All lesioned animals exhibited <10% residual staining in the dopamine-denervated striatum and were thus included in the study.

MicroPET

Ketamine Studies—In all 41 animals (20 6-OHDA, 21 Sham), anesthesia was induced with an intraperitoneal injection of ketamine (100 mg/kg)/xylazine (10 mg/kg) cocktail 15 minutes after receiving a subcutaneous injection of saline or levodopa. Once absence of reflexes was confirmed, the lateral tail vein was catheterized with a 24-gauge needle with attached polyethylene tubing for injection of $H_2\,^{15}O$. Two 25-gauge intraperitoneal butterfly catheter lines were secured with transpore tape: on the right intraperitoneal cavity for FDG injection, and on the left cavity for ketamine/xylazine bolus anesthesia maintenance. Anesthesia was maintained as needed (0.3 mL/kg). After lines were secured, the animal was placed on the scanner platform, with the head centered in the camera field of view; the animal position was maintained until completion of both scans. For CBF scans, 37–74 MBq of $H_2\,^{15}O$ tracer was injected into the lateral tail vein line and a 4-minute emission scan was immediately acquired. A between-scan interval of 10-minutes was allowed for [^{15}O] decay prior to the start of FDG scanning for concurrent CMR measurement. To this end, 37–74 MBq of FDG was injected in the previously secured right intraperitoneal line; a 45-minute uptake period was allowed, prior to the acquisition of a 10-minute emission scan which was followed by a 4-minute transmission scan. At conclusion of both scans, animals were allowed to recover on a clean cage until regaining the righting reflex.

Isoflurane Studies—In 15 animals (8 6-OHDA, 7 Sham), anesthesia was induced with 2.5% isoflurane in 100% oxygen, via a breathing mask, 15 minutes after a subcutaneous saline or levodopa injection. Anesthesia delivery remained constant throughout the scanning session. The scanning procedure was otherwise the same as that described for the ketamine scanning sessions, with the exception that only one catheter line was secured on the right intraperitoneal cavity for FDG delivery. All images were corrected for attenuation and reconstructed using an iterative reconstruction approach utilizing the 3D ordered subsets-expectation maximization (3D OSEM)/maximum *a priori* (MAP) algorithm.

Data Analysis

Data Processing—Imaging data processing was performed using PMOD (PMOD Technologies, Zurich, Switzerland) and SPM5 (Wellcome Department of Cognitive Neurology, London, UK) with SPMMOUSE (http://www.spmmouse.org) implemented in Matlab 6.1 (Mathworks, Sherborn, MA). The FDG scans from each subject were manually aligned in PMOD to an FDG template (Schiffer et al., 2007). For each animal, all transformations from FDG scan alignments were directly applied to the corresponding $H_2\ ^{15}O$ scans from the same

Unbiased whole brain voxel-wise searches were conducted in the 6-OHDA lesioned animals for regions with significant levodopa-mediated CBF/CMR dissociation (Hirano et al., 2008). This analysis identified regions in which significant tracer (CBF/CMR) × condition (levodopa/saline) interaction effects were present in the globally-normalized scan data. Scans from the two anesthesia protocols were analyzed separately. In both analyses, the resulting maps were thresholded at $p<0.001$ (peak voxel, uncorrected) and were considered significant at $p<0.05$ (corrected for cluster extent), corresponding to approximately $k=50$ voxels for each data set. Volumes-of-interest (VOIs) were used post-hoc to evaluate the individual data from each significant cluster in the 6-OHDA and sham-lesioned animals. CBF and CMR values for each VOI were ratio-normalized by the corresponding global whole brain value for each scan. For each significant VOI, globally normalized CBF and CMR values were measured for the individual animals in each group and treatment condition (sham saline (SS), sham levodopa (SLD), lesion saline (LS) and lesion levodopa (LLD)) scanned under the two anesthetic protocols (ketamine and isoflurane). For the ketamine protocol, tracer (CBF/CMR) × condition (LLD/LS or SLD/SS) interaction effects were evaluated in the post-hoc VOI data using RMANOVA (with tracer as the repeated measure) with Bonferroni correction. For the isoflurane protocol, interaction effects in the VOI data were evaluated using 2×2 RMANOVA (with tracer × condition as the repeated measures) with appropriate Bonferroni tests.

In regions with significant interaction effects, we also computed a regional dissociation index (DI) defined as the change in functional activity of blood flow ($CBF_{levodopa} - CBF_{saline}$) minus the change in metabolism ($CMR_{levodopa} - CMR_{saline}$), or ($\Delta CBF - \Delta CMR$). We only computed this index for isoflurane regions, where levodopa and saline conditions were obtained within the same animal. For each region, a DI value of 0 indicated equal treatment-mediated changes in functional activity for CBF and CMR scan data. Positive DI values indicated greater treatment-mediated changes in blood flow relative to metabolism ($\Delta CBF > \Delta CMR$), whereas negative values indicated the opposite ($\Delta CBF < \Delta CMR$). Differences in DI across lesion and sham groups were assessed with Student's *t*-test.

Anesthetic Comparison—To explore differences in tracer × condition interaction effects across anesthetic protocols, we lowered the voxel-level threshold to $p<0.01$, uncorrected. We determined whether the significant clusters identified under ketamine/xylazine anesthesia exhibited similar levodopa-mediated dissociation effects when evaluated under the same pharmacologic conditions in the isoflurane data. Thus, globally normalized CBF and CMR values were measured in the ketamine scans at VOI coordinates corresponding to the

significant clusters identified in the isoflurane data. Likewise, in the isoflurane scans, normalized CBF and CMR values were measured in the significant clusters identified in the ketamine data. Comparisons of CBF and CMR values between anesthetic groups were conducted using Student's *t*-tests.

Statistical analysis was performed using Statistical Analysis System (SAS), version 9.3 (SAS, Cary, NC). The results were considered significant at $p<0.05$.

Results

Flow-Metabolism Dissociation

Group Comparisons—We analyzed CBF and CMR scan data from 20 6-OHDA lesioned animals (lesion saline (LS): n=9; lesion levodopa (LLD): n=11) and 21 sham animals (sham saline (SS): n=10; sham levodopa (SLD): n=11) studied under ketamine anesthesia (Fig. 1A; Table 1) in which there was a significant difference in CBF and CMR responses for the LS and LLD groups. This region was localized to the striatum of the lesioned hemisphere. Analysis of individual animal CBF and CMR values for this cluster measured in the LS and LLD groups (Fig. 1B, *left*) was remarkable for a significant tracer × group interaction effect ($F_{(1,18)}=16.8$, p=0.001; RMANOVA). Further analysis of the data from this region showed that levodopa-treated 6-OHDA animals (Fig. 1B, *left*) exhibited relatively increased CBF (p=0.01) and lower CMR (p<0.001, post-hoc Bonferroni tests) compared to their saline treated counterparts. By contrast, in the SS and SLD group (Fig. 1B, *right*), no significant tracer × group interaction effect ($F_{(1,19)}=0.88$, p=0.36; RMANOVA) was present in this region to suggest dissociation of CBF and CMR levodopa responses.

Treatment-Mediated Changes—A subgroup of eight 6-OHDA lesioned and seven sham animals from the ketamine study additionally underwent dual-tracer microPET under isoflurane anesthesia. In each of these animals, CBF and CMR scans were obtained following both levodopa and saline administration. In the 6-OHDA animals, whole brain voxel searches revealed several areas of significant levodopa-mediated CBF/CMR dissociation (Table 2) in the lesioned (right) hemisphere. The largest cluster (k=99 voxels) was localized to globus pallidus (GP) (Fig. 2A) extending into the adjacent caudal striatum. Analysis of the VOI data from this region (Fig. 2B, *left*) disclosed a significant tracer × condition interaction effect ($F_{(1,7)}=14.11$, p=0.007; 2×2 RMANOVA), with a levodopa-mediated increase in CBF (p=0.02). While, in this region, seven of the eight 6-OHDA animals exhibited a concurrent decline in CMR following levodopa administration, the magnitude of the overall change was not significant (p=0.23). By contrast, in the sham group (Fig. 2B, *right*) levodopa was not associated with significant CBF/CMR dissociation in this region ($F_{(1,6)}=0.5$, p=0.50).

A smaller area (k=82 voxels) of levodopa-mediated CBF/CMR dissociation was detected (Fig. 3A) in the right enteropeduncular (EP) nucleus of the 6-OHDA animals scanned under the isoflurane protocol. The VOI data from this region exhibited a significant tracer × condition interaction effect ($F_{(1,7)}=18.81$, p=0.003; 2×2 RMANOVA), with levodopa-mediated increases in local CBF (Fig. 3B, *left*) in all eight animals (p=0.002). Consistent levodopa-mediated CMR change in this region were not observed (p=0.99) in the 6-OHDA

lesioned animals. As above, treatment-mediated CBF/CMR dissociation (Fig. 3B, *right*) was not present in the sham animals ($F_{(1,6)}$=1.36, p=0.29). Lastly, a small region (k=61 voxels) of significant levodopa-mediated dissociation was observed (Fig. 4A) in the right auxiliary motor cortex (M2) of the 6-OHDA animals. A highly significant tracer × condition interaction effect ($F_{(1,7)}$=37.69, p=0.0005) was present in this region (Fig. 4B, *left*), with consistent increases in CBF (p=0.02) and declines in CMR (p=0.0008) in this group of animals. Analogous levodopa-mediated dissociation effects (Fig. 4B, *right*) were not seen in the sham group ($F_{(1,6)}$=0.81, p=0.40).

Anesthetic Comparison

To explore the basis for the difference in the location of the dissociation regions identified under the two anesthetic protocols, we relaxed the threshold employed for the respective whole brain searches (see Methods). Accordingly, at a hypothesis-testing threshold of p<0.01 (uncorrected), we noted that the border of the striatal cluster that was previously identified under ketamine (Table 1) migrated posteriorly into its isoflurane counterpart in the GP region. That said, relaxation of the significance threshold did not influence the previously identified isoflurane cluster (Table 2), i.e., there was no reciprocal shift of its border anteriorly toward its ketamine counterpart in the striatum. This difference suggests that the localized dissociation effects identified under ketamine incorporate anesthetic-related changes not seen with isoflurane. Further analysis revealed that as a potent NMDA antagonist, ketamine may alter baseline regional activity in a manner not evident with non-specific anesthetic agents such as isoflurane. Indeed, baseline CBF values measured in the striatal cluster (1.8, −0.2, −5.0 mm) were relatively lower in animals anesthetized with ketamine compared to isoflurane (ketamine: 1.26±0.24 (mean±SD); isoflurane: 1.46±0.20, p=0.068; Student's *t*-test).

Discussion

Metabolic and Vasomotor Responses to Levodopa Therapy

We found that 6-OHDA lesioned animals anesthetized with either ketamine/xylazine or isoflurane exhibited significant dissociation of CBF and CMR responses to acute levodopa injection in the basal ganglia. While this phenomenon has been described previously in living PD patients receiving intravenous levodopa infusion (Hirano et al., 2008), this study is the first to demonstrate its presence *in vivo* in the experimental 6-OHDA rat model. We also found that significant levodopa-mediated dissociation was evident under anesthesia, whether induced with ketamine/xylazine or isoflurane. With both protocols, significant dissociation of CBF and CMR responses to levodopa in the basal ganglia was observed in 6-OHDA lesioned hemispheres. That said, the localization of levodopa-mediated CBF/CMR dissociation within the basal ganglia differed somewhat for the two anesthetic regimens. With ketamine/xylazine, significant dissociation was restricted to the caudal medial striatum whereas with isoflurane, the region extended caudally into the ventral GP. Moreover, two additional significant regions in the ipsilateral EP and M2 were identified in the isoflurane data; dissociation effects in these regions were less pronounced than for the GP. In aggregate, the microPET findings accord well with published autoradiographic findings (Ohlin et al., 2012). We note, however, that the apparent sensitivity of the isoflurane study to

these changes is not necessarily attributable to the agent chosen. Rather, the analytical design employed in the isoflurane experiments may have facilitated the detection of significant dissociation effects in a manner not possible in the ketamine study. In the latter, levodopa and saline were administered to separate groups of animals, whereas the isoflurane animals were scanned with the two radiotracers under both pharmacologic conditions. The within-subject design used for the isoflurane study reduced the contribution of between-subject error in the estimation of the relevant interaction effects.

Notably, to identify areas of dissociation under ketamine/xylazine or isoflurane, we conducted unbiased voxel-wise searches across the entire brain volume for regions with significant treatment (levodopa, saline) × tracer (CBF/CMR) interaction effects. As demonstrated in the human (Hirano et al., 2008), areas with significantly dissociated CBF and CMR responses to levodopa are also found to express aromatic L-amino acid decarboxylase (Garcia-Cabezas et al., 2007; Smith and Kieval, 2000). Indeed, decarboxylation of levodopa to dopamine is a necessary first step in mediating these responses. Similarly, regardless of the anesthetic used, dissociation was present only in dopamine-denervated hemispheres. Indeed, dissociated CBF and CMR responses to levodopa were not detected in the intact contralateral hemispheres of the 6-OHDA lesioned animals or in their sham-operated counterparts. This accords well with prior human and animal data linking aberrant levodopa responses to underlying dopaminergic denervation (Cenci and Lundblad, 2006; Hirano et al., 2008; Mosharov et al., 2015; Stanic et al., 2003).

Consistent with an earlier autoradiographic study conducted in the 6-OHDA rat (Ohlin et al., 2012), the microPET data indicate that chronic levodopa exposure is not a *sine qua non* for CBF/CMR dissociation to take place in response to acute injection of the drug. Indeed, in the current study the animals had not been previously exposed to chronic levodopa or other dopaminergic agents. Even so, acute levodopa injection gave rise to CBF/CMR dissociation in nearly all 6-OHDA animals scanned in both the saline and levodopa conditions. As in the autoradiographic study, hemodynamic (CBF) response to levodopa tended to overshadow concurrent local metabolic reductions as the main “driver” of levodopa-mediated dissociation in the 6-OHDA animal model. This acute effect of levodopa administration is likely mediated through direct engagement of dopamine receptors on microvessel-associated cells (Afonso-Oramas et al., 2014; Edvinsson et al., 1985).

Flow-Metabolism Dissociation and Complications of Levodopa Therapy

Recent studies have suggested that levodopa-mediated CBF/CMR dissociation is accentuated by chronic dopaminergic therapy for PD and that this phenomenon may play a role in the pathogenesis of LID and other long-term complications of treatment (Cenci, 2014; Hirano et al., 2008; Jourdain et al., 2015). Molecular studies conducted in the 6-OHDA rat have demonstrated that chronic levodopa administration results in microvascular responses such as VEGF (vascular endothelial growth factor) upregulation, endothelial proliferation, increased blood vessel length, nestin staining, and local BBB disruption (Lindgren et al., 2009; Ohlin et al., 2011; Westin et al., 2006). These findings were observed only in association to LID, implicating the microvascular changes in the development of this side effect of chronic levodopa therapy. Interestingly, based on their autoradiographic data,

Ohlin et al. (2012) suggested that analogous dissociation effects were also present in the basal ganglia and motor cortex of chronically levodopa-treated animals who developed drug-induced dyskinesias. While significant increases in CBF with acute levodopa administration were also seen in drug-naïve animals, the magnitude of responses was larger in the chronically treated sample. Given that in the autoradiographic study, levodopa-mediated CBF increase was evident in anesthetized animals in which dyskinesia movements were suppressed, it is unlikely that the observed changes were a consequence of the motor manifestations. However, to understand the precise mechanisms underlying the abnormal movements themselves, simultaneous measurements of local CBF and CMR will be needed both at baseline and during the induction of LID by medication. This information can only be gained through the study of 6-OHDA-lesioned rodents who have been chronically treated with levodopa/carbidopa (Ohlin et al., 2011). We plan to use the dual-tracer microPET approach described in the current study to examine the relationship between levodopa-mediated dissociation and LID in these animals. We will also use this approach to explore the relationship between dissociation and changes in BBB permeability occurring concurrently in the same brain regions.

Conclusion

Dissociation of metabolic and vasomotor responses has been recently reported in PD patients receiving an acute levodopa challenge. In particular, this phenomenon is likely exaggerated in PD patients developing LID following chronic levodopa treatment. The current data demonstrate the feasibility of using dual-tracer microPET for *in vivo* studies of flow-metabolism dissociation in the 6-OHDA rat model, with or without the induction of dyskinesias. Moreover, the data show that an experimentally induced dopaminergic denervation is sufficient to reproduce the abnormal hemodynamic responses to levodopa previously observed in PD patients.

Acknowledgments

Funding

This work was supported by the National Institute of Neurological Disorders and Stroke Morris K. Udall Center of Excellence for Parkinson's Disease Research at The Feinstein Institute for Medical Research (P50 NS071675 to D.E.). The content is solely the responsibility of the authors and does not necessarily represent the official views of the National Institute of Neurological Disorders and Stroke or the National Institutes of Health. The sponsor did not play a role in study design, collection, analysis and interpretation of data, writing of the report or in the decision to submit the paper for publication.

The authors are thankful to Ms. Yoon Young Choi and Ms. Toni Fitzpatrick for valuable editorial assistance and to Dr. An Vo for helpful discussions. Special thanks to Mr. David Bjelke, Mr. Spiro Kavathas, Mr. Ralph Matacchieri and Mr. Abbas Ali for radiotracer support.

Abbreviations

BBB	blood brain barrier
6-OHDA	6-hydroxydopamine
PD	Parkinson's disease

$H_2{}^{15}O$	^{15}O-water
FDG	^{18}F-fluorodeoxyglucose
CBF	cerebral blood flow
CMR	cerebral metabolic rate for glucose
GP	globus pallidus
LID	levodopa-induced dyskinesia
VOI	volume-of-interest
DI	dissociation index
EP	enteropeduncular nucleus
M2	auxiliary motor cortex

References

Afonso-Oramas D, et al. Striatal vessels receive phosphorylated tyrosine hydroxylase-rich innervation from midbrain dopaminergic neurons. Front Neuroanat. 2014; 8:84. [PubMed: 25206324]

Asanuma K, et al. Network modulation in the treatment of Parkinson's disease. Brain. 2006; 129:2667–2678. [PubMed: 16844713]

Cavazzuti M, et al. Ketamine effects on local cerebral blood flow and metabolism in the rat. J Cereb Blood Flow Metab. 1987; 7:806–811. [PubMed: 3121648]

Cenci MA. Presynaptic Mechanisms of l-DOPA-Induced Dyskinesia: The Findings, the Debate, and the Therapeutic Implications. Front Neurol. 2014; 5:242. [PubMed: 25566170]

Cenci MA, Lundblad M. Post- versus presynaptic plasticity in L-DOPA-induced dyskinesia. J Neurochem. 2006; 99:381–392. [PubMed: 16942598]

Edvinsson L, et al. Vasomotor response of cerebral blood vessels to dopamine and dopaminergic agonists. Adv Neurol. 1978; 20:85–96. [PubMed: 676925]

Edvinsson L, et al. Vasomotor responses of cerebral arterioles in situ to putative dopamine receptor agonists. Br J Pharmacol. 1985; 85:403–410. [PubMed: 3896363]

Filosa JA, et al. Beyond neurovascular coupling, role of astrocytes in the regulation of vascular tone. Neuroscience. 2016; 26:96–109.

Garcia-Cabezas MA, et al. Distribution of the dopamine innervation in the macaque and human thalamus. Neuroimage. 2007; 34:965–984. [PubMed: 17140815]

Guell A, et al. Effects of a dopaminergic agonist (piribedil) on cerebral blood flow in man. J Cereb Blood Flow Metab. 1982; 2:255–257. [PubMed: 7076737]

Hirano S, et al. Dissociation of metabolic and neurovascular responses to levodopa in the treatment of Parkinson's disease. J Neurosci. 2008; 28:4201–4209. [PubMed: 18417699]

Jourdain VA, et al. Levodopa-induced changes in neurovascular reactivity in Parkinson's disease. Mov Disord. 2015; 30:S11.

Leenders KL, et al. The effects of L-DOPA on regional cerebral blood flow and oxygen metabolism in patients with Parkinson's disease. Brain. 1985; 108(Pt 1):171–191. [PubMed: 3978397]

Lindgren HS, et al. Differential involvement of D1 and D2 dopamine receptors in L-DOPA-induced angiogenic activity in a rat model of Parkinson's disease. Neuropsychopharmacology. 2009; 34:2477–2488. [PubMed: 19606087]

McCulloch J, Edvinsson L. Cerebral circulatory and metabolic effects of piribedil. Eur J Pharmacol. 1980; 66:327–337. [PubMed: 7418723]

Mosharov EV, et al. Presynaptic effects of levodopa and their possible role in dyskinesia. Mov Disord. 2015; 30:45–53. [PubMed: 25450307]

Ohlin KE, et al. Vascular endothelial growth factor is upregulated by L-dopa in the parkinsonian brain: implications for the development of dyskinesia. Brain. 2011; 134:2339–2357. [PubMed: 21771855]

Ohlin KE, et al. Impact of L-DOPA treatment on regional cerebral blood flow and metabolism in the basal ganglia in a rat model of Parkinson's disease. Neuroimage. 2012; 61:228–239. [PubMed: 22406356]

Ruscher K, et al. Levodopa treatment improves functional recovery after experimental stroke. Stroke. 2012; 43:507–513. [PubMed: 22096034]

Schiffer WK, et al. Optimizing experimental protocols for quantitative behavioral imaging with 18F-FDG in rodents. J Nucl Med. 2007; 48:277–287. [PubMed: 17268026]

Smith Y, Kieval JZ. Anatomy of the dopamine system in the basal ganglia. Trends Neurosci. 2000; 23:S28–S33. [PubMed: 11052217]

Stanic D, et al. Changes in function and ultrastructure of striatal dopaminergic terminals that regenerate following partial lesions of the SNpc. J Neurochem. 2003; 86:329–343. [PubMed: 12871574]

Toda N. Influence of dopamine and noradrenaline on isolated cerebral arteries of the dog. Br J Pharmacol. 1976; 58:121–126. [PubMed: 974370]

Westin JE, et al. Endothelial proliferation and increased blood-brain barrier permeability in the basal ganglia in a rat model of 3,4-dihydroxyphenyl-L-alanine-induced dyskinesia. J Neurosci. 2006; 26:9448–9461. [PubMed: 16971529]

Winkler C, et al. L-DOPA-induced dyskinesia in the intrastriatal 6-hydroxydopamine model of parkinson's disease: relation to motor and cellular parameters of nigrostriatal function. Neurobiol Dis. 2002; 10:165–186. [PubMed: 12127155]

Highlights

- *In vivo* measurements of cerebral blood flow and metabolism in the 6-OHDA rat model.
- Dissociated response of blood flow and metabolism to acute levodopa challenge.
- Levodopa response driven by significant increases in blood flow.
- MicroPET approach will have utility for studying levodopa-induced dyskinesias.

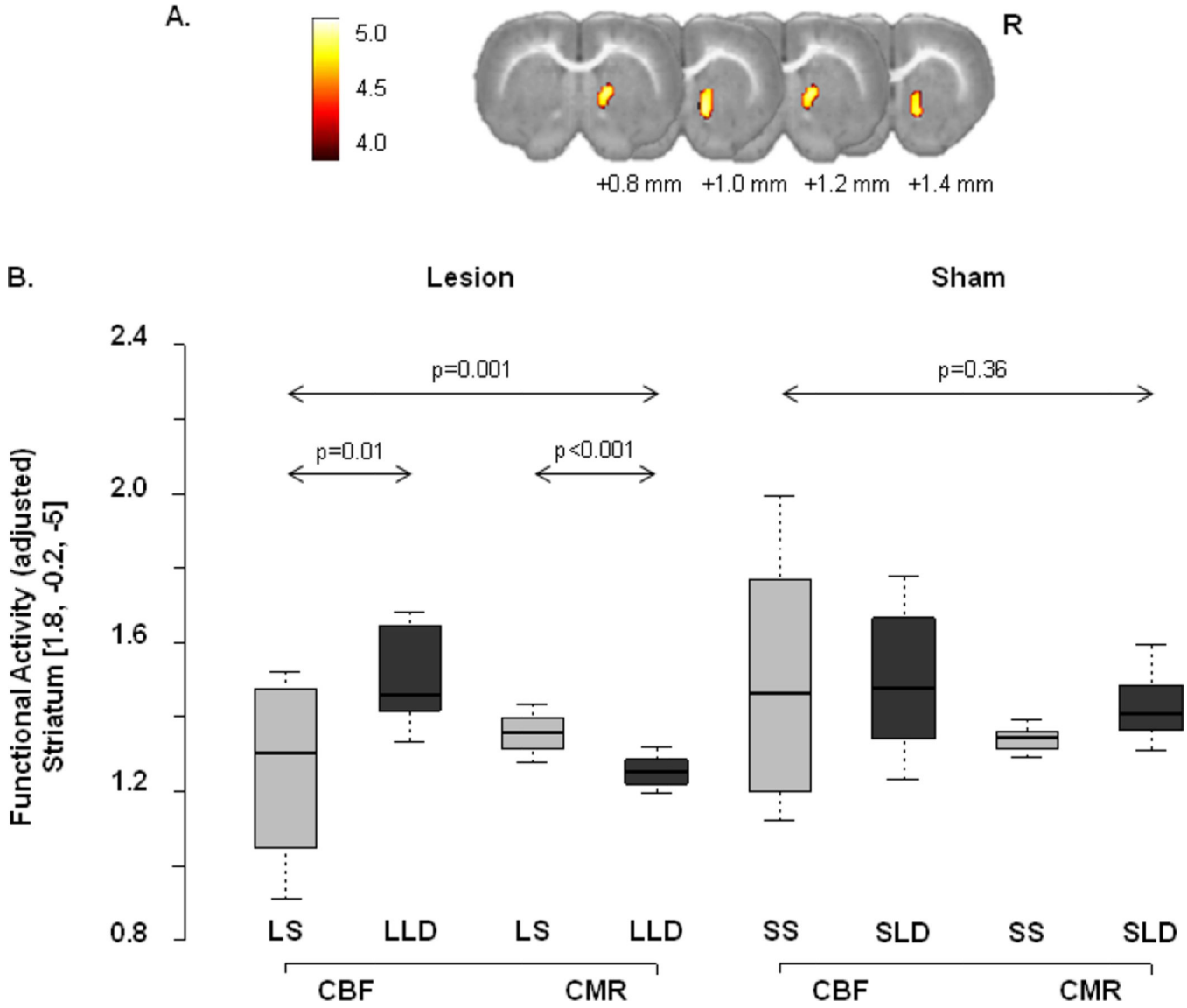

Figure 1.

(A) Maps of CBF and CMR generated in unilaterally lesioned 6-OHDA rats who underwent sequential $H_2{}^{15}O$ and FDG PET under ketamine/xylazine anesthesia. Whole brain voxel-wise searches were conducted to identify discrete regions in which CBF and CMR were dissociated in response to levodopa vs. saline (see text). The analysis disclosed a single region with significant dissociation, which was localized to the striatum (*yellow*) of the lesioned (right) hemisphere. **(B)** Box-and-whisker plot of CBF and CMR values in this region. *Left:* Significant CBF/CMR dissociation was seen in 6-OHDA lesioned rats ($F_{(1,18)}$=16.8, p=0.001, tracer × group interaction effect; RMANOVA) with increased CBF (p=0.01) and reduced CMR (p<0.001; post-hoc Bonferroni tests) in animals receiving levodopa (*dark gray bars*) compared to saline (*light gray bars*). *Right:* Analogous dissociation effects were not seen in sham-lesioned animals. [LLD: 6-OHDA lesioned animals receiving levodopa; LS: 6-OHDA lesioned animals receiving saline; SLD: sham-lesioned animals receiving levodopa SS: sham-lesioned animals receiving saline.]

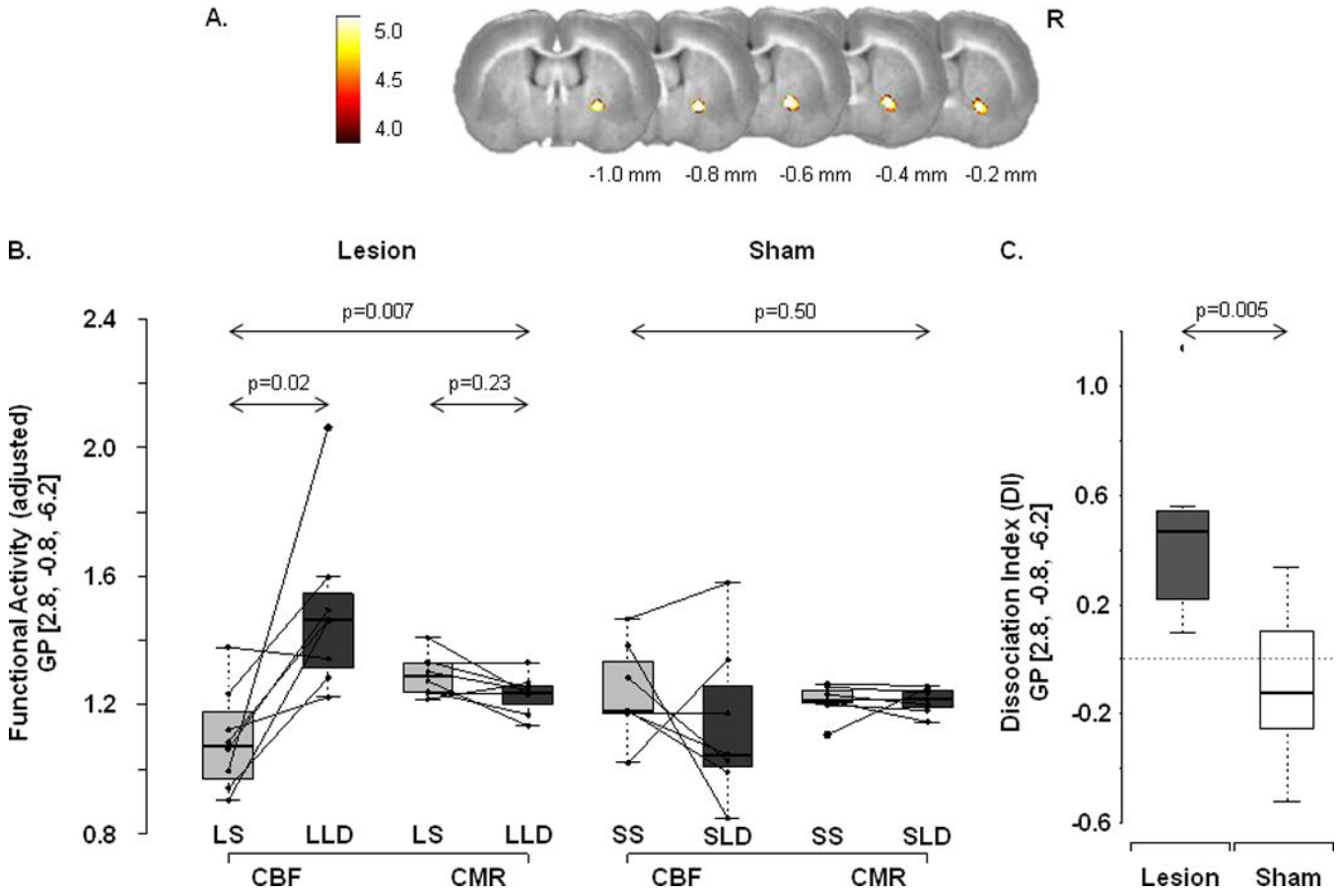

Figure 2.

(A) A subset of the animals studied under ketamine/xylazine underwent additional dual-tracer microPET under isoflurane anesthesia. In this group, levodopa and saline were administered to the same animals in separate scanning sessions (see text). Analogous voxel-wise searches revealed a discrete region with dissociated CBF and CMR responses to the levodopa in the globus pallidus (GP) (*yellow*) of the lesioned (right) cerebral hemisphere. **(B)** Box-and-whisker plot of CBF and CMR values in this region. *Left*: Significant CBF/CMR dissociation was seen 6-OHDA lesioned rats ($F_{(1,7)}$=14.11, p=0.007, tracer × condition interaction effect; RMANOVA) with increased CBF (p=0.02) and declining CMR (p=0.23) in the saline vs. levodopa conditions. *Right*: Analogous changes were not seen in the sham-lesioned animals. **(C)** Comparison of levodopa-mediated CBF/CMR dissociation measured in the GP region described in **(A)** for the 6-OHDA and sham-lesioned animals (see text). The dissociation index (DI) (see Materials and Methods) computed in each of the 6-OHDA and sham-lesioned animals revealed a significant difference in the levodopa-mediated dissociation response for the two groups (p=0.005, Student's *t*-test). [LLD: 6-OHDA lesioned animals receiving levodopa; LS: 6-OHDA lesioned animals receiving saline; SLD: sham-lesioned animals receiving levodopa; SS: sham-lesioned animals receiving saline.]

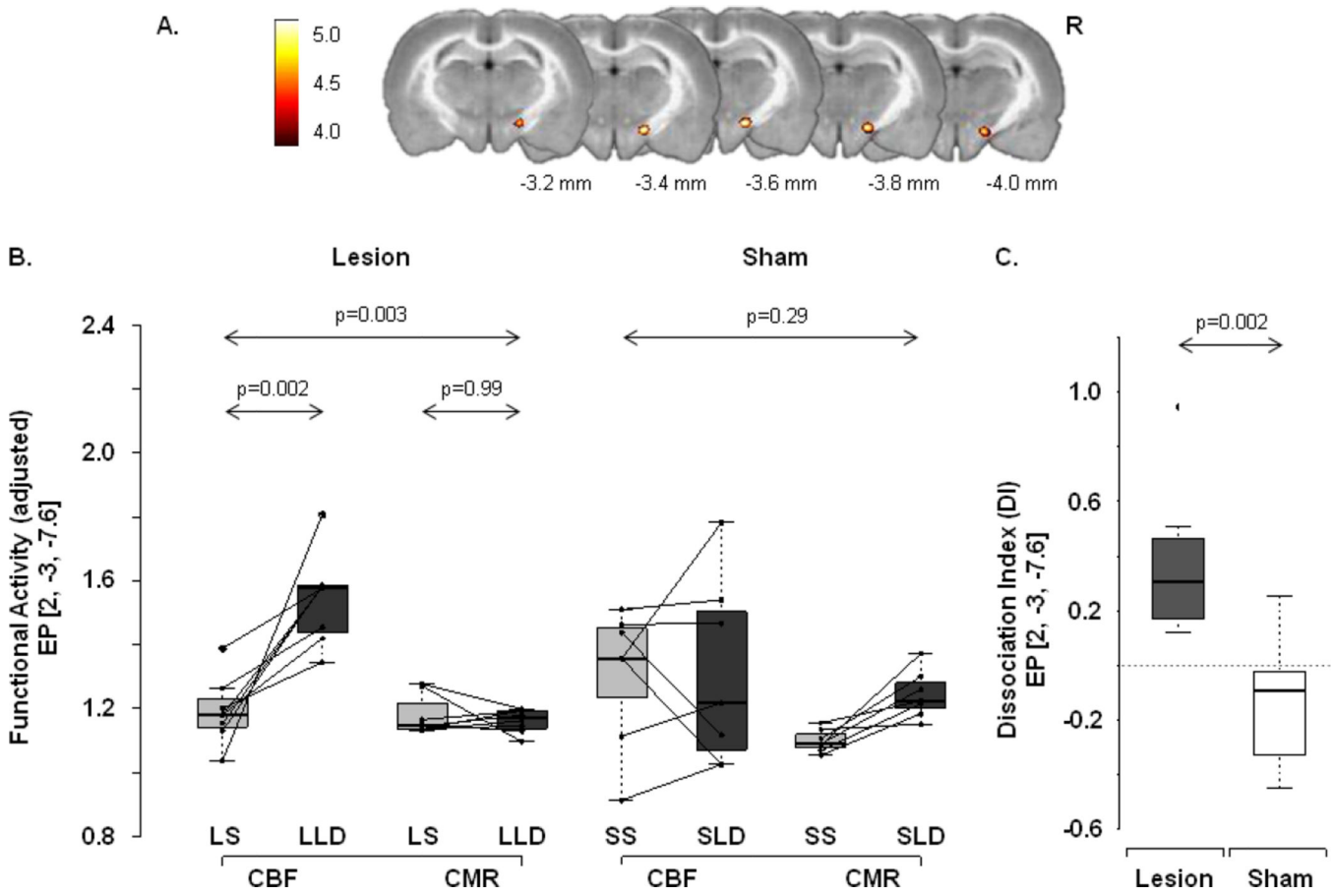

Figure 3.

(A) Voxel-wise interrogation of the CBF and CMR scans acquired in the 6-OHDA lesioned animals studied under isoflurane anesthesia revealed an additional area of significant levodopa-mediated dissociation in the ipsilateral (right) enteropeduncular (EP) nucleus. **(B)** Box-and-whisker plot of CBF and CMR values in this region. *Left*: Significant CBF/CMR dissociation was seen 6-OHDA lesioned rats ($F_{(1,7)}$=18.81, p=0.003, tracer × condition interaction effect; RMANOVA) with increased CBF (p=0.002) and declining CMR (p=0.99) in the saline vs. levodopa conditions. *Right*: Analogous changes were not seen in the sham-lesioned animals. **(C)** Comparison of levodopa-mediated CBF/CMR dissociation measured in the EP region described in **(A)** for the 6-OHDA and sham-lesioned animals (see text). The dissociation index (DI) (see Materials and Methods) computed in each of the 6-OHDA and sham-lesioned animals revealed a significant difference in the levodopa-mediated dissociation response for the two groups (p=0.002, Student's *t*-test). [LLD: 6-OHDA lesioned animals receiving levodopa; LS: 6-OHDA lesioned animals receiving saline; SLD: sham-lesioned animals receiving levodopa; SS: sham-lesioned animals receiving saline.]

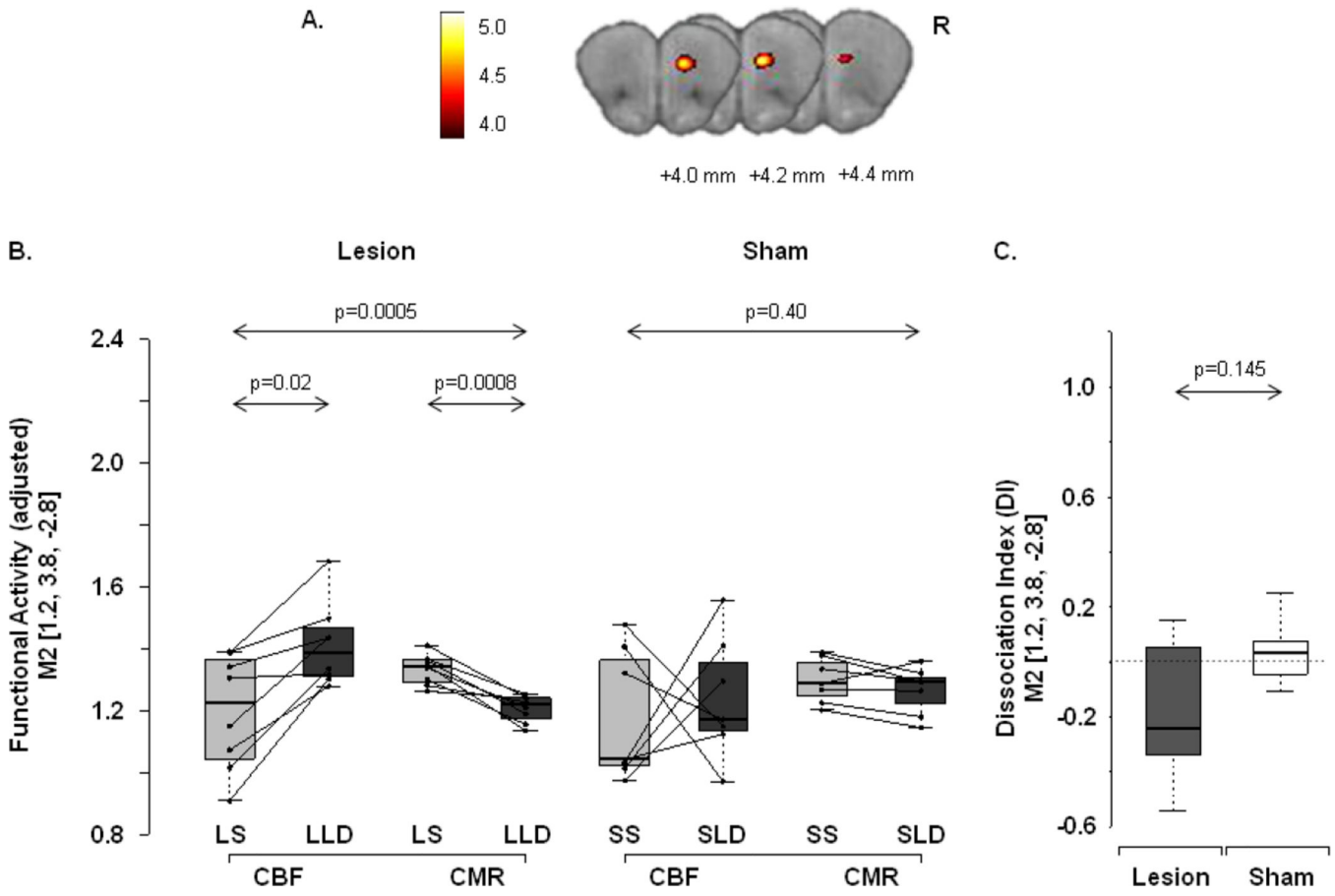

Figure 4.

(A) A third area of significant levodopa-mediated CBF/CMR dissociation was identified in the 6-OHDA animals studied under isoflurane anesthesia. This region was localized to the auxiliary motor cortex (M2) of the lesioned hemisphere. **(B)** Box-and-whisker plot of CBF and CMR values in this region. *Left*: Significant CBF/CMR dissociation was seen 6-OHDA lesioned rats ($F_{(1,7)}$=37.69, p=0.0005, tracer × condition interaction effect; RMANOVA) with increased CBF (p=0.02) and declining CMR (p=0.0008) in the saline vs. levodopa conditions. *Right*: Analogous changes were not seen in the sham-lesioned animals. **(C)** In this region, however, no significant difference was seen for dissociation index values measured in 6-OHDA and sham-lesioned animals (p=0.145, Student's *t*-test). [LLD: 6-OHDA lesioned animals receiving levodopa; LS: 6-OHDA lesioned animals receiving saline; SLD: sham-lesioned animals receiving levodopa; SS: sham-lesioned animals receiving saline.]

Table 1

Brain region with significant flow-metabolism dissociation after a levodopa challenge under ketamine/xylazine anesthesia

	Coordinates			Cluster Size	Z_{max}	p-value*	CMR†		CBF‡		Tracer ×Condition RMANOVA	
	X	Y	Z				Saline	Levodopa	Saline	Levodopa	F-value	p-value
Striatum (R)	1.8	−0.2	−5	179	4.01	0.001	1.36(0.04)	1.25(0.04)	1.26(0.24)	1.51(0.13)	$F_{(1,18)}$=16.80	0.001
Striatum (L)							1.35(0.03)	1.41(0.06)	1.40(0.15)	1.63(0.19)	$F_{(1,18)}$=3.781	0.068

*Significant flow-metabolism dissociation (SPM interaction analysis), p=0.001, uncorrected

†Globally normalized CMR for glucose [mean(SD)] in each VOI (see Materials and Methods)

‡Globally normalized CBF [mean(SD)] in each VOI (see Materials and Methods)

CMR, cerebral metabolic rate; CBF, cerebral blood flow

Table 2

Brain regions with significant flow-metabolism dissociation after a levodopa challenge under isoflurane anesthesia

	Coordinates			Cluster Size	Z_{max}	p-value*	CMR†		CBF‡		Tracer ×Condition RMANOVA	
	X	Y	Z				Saline	Levodopa	Saline	Levodopa	F-value	p-value
GP (R)	2.8	−0.8	−6.2	99	4.17	0.003	1.29(0.07)	1.23(0.06)	1.09(0.16)	1.49(0.26)	$F_{(1,7)}$=14.11	0.0071
GP (L)							1.27(0.05)	1.25(0.04)	1.28(0.26)	1.11(0.27)	$F_{(1,7)}$=1.64	0.2410
EP (R)	2	−3	−7.6	82	4.40	0.006	1.18(0.06)	1.16(0.03)	1.19(0.10)	1.55(0.14)	$F_{(1,7)}$=18.81	0.0034
EP (L)							1.11(0.04)	1.13(0.05)	1.21(0.27)	1.24(0.13)	$F_{(1,7)}$=0.01	0.9935
M2 (R)	1.2	3.8	−2.8	61	4.17	0.016	1.33(0.05)	1.21(0.04)	1.20(0.18)	1.41(0.13)	$F_{(1,7)}$= 37.69	0.0005
M2 (L)							1.31(0.07)	1.23(0.05)	1.25(0.23)	1.24(0.22)	$F_{(1,7)}$=0.36	0.5697

*Significant flow-metabolism dissociation (SPM interaction analysis), p=0.001, uncorrected

†Globally normalized CMR for glucose [mean(SD)] in each VOI (see Materials and Methods)

‡Globally normalized CBF [mean(SD)] in each VOI (see Materials and Methods)

CMR, cerebral metabolic rate; CBF, cerebral blood flow; GP, globus pallidus; EP, enteropeduncular nucleus; M2, auxiliary motor cortex